Thin Solid Films 575 (2015) 42–46

Contents lists available at ScienceDirect

Thin Solid Films

journal homepage: www.elsevier.com/locate/tsf

Degradation of a tantalum filament during the hot-wire CVD of silicon nitride thin films

C.J. Oliphant [a,b], C.J. Arendse [a,*], T.F.G. Muller [a], W.A. Jordaan [b], D. Knoesen [a]

[a] Department of Physics, University of the Western Cape, Private Bag X17, Bellville 7535, South Africa
[b] National Metrology Institute of South Africa, Private Bag X34, Lynwood Ridge, Pretoria 0040, South Africa

ARTICLE INFO

Available online 12 October 2014

Keywords:
Hot-wire deposition
Electron backscatter diffraction
Hardness
Filament degradation

ABSTRACT

Electron backscatter diffraction revealed that during the hot-wire deposition of silicon nitride, a tantalum filament partially transformed to some of its nitrides and silicides. The deposition of an encapsulating silicon nitride layer occurred at the cooler filament ends. Time-of-flight secondary ion mass spectroscopy disclosed the presence of hydrogen, nitrogen and silicon containing ions within the aged filament bulk. Hardness measurements revealed that the recrystallized tantalum core experienced significant hardening, whereas the silicides and nitrides were harder but more brittle. Crack growth, porosity and the different thermal expansion amongst the various phases are all enhanced at the hotter centre regions, which resulted in failure at these areas.

1. Introduction

The hot-wire chemical vapour deposition (HWCVD) technique has shown great potential as a viable alternative to plasma enhanced CVD (PECVD) for the mass production of silicon nitride (SiN_x) [1,2]. The most striking feature, however, of HWCVD is its superior SiN_x growth rates compared to PECVD [2] and the absence of ion bombardment during the deposition. Despite the obvious advantage that the heated filament grants to HWCVD, few studies have been reported on the interaction of nitrogen-containing gases and the filament. In this study we used tantalum (Ta) filaments heated to 1600 °C in a $NH_3/SiH_4/H_2$ ambient to synthesise SiN_x layers at very promising growth rates despite the relative low deposition pressure and precursor gas flow rates used. Regardless of these promising deposition conditions and the filament pre-treatment, as suggested by Knoesen et al. [3], the Ta filament experienced failure at the end of the deposition after a total of five 1 hour depositions. The origins for the filament degradation are identified based on elemental, microstructural and mechanical properties of the aged filaments.

2. Experimental details

A Ta-filament with a diameter of 244.8 ± 10.0 μm and a length of ~1 m, prepared according to a standard process [3], was used to synthesise SiN_x thin films at a filament temperature of 1600 °C using an MVSystems® HWCVD reactor. The deposition pressure, substrate temperature, SiH_4 flow rate and H_2 flow rate were fixed to 150 μbar, 240 °C, 2 sccm and 27 sccm, respectively. At these deposition conditions, we showed that SiN_x films with a nitrogen to a silicon ratio of up to 1.18, a deposition rate of 24 nm/min, hydrogen content of 9.14 at.%, surface roughness of ~0.15 nm and a refractive index of ~1.9 can be synthesised [4].

The only deposition variable was the NH_3 flow rate, which was changed from 1 to 3 sccm (in increments of 0.5 sccm). The same filament was used for all the SiN_x depositions and lasted for five 1 hour depositions. The Ta-filament was subsequently carefully removed from the HWCVD reactor in order to limit any mechanical disturbances. Multiple regions were sampled along the length of the filament and metallographically prepared for SEM analysis. The microstructure of the cross-sections was analysed using a LEO 1525 field-emission gun scanning electron microscope (FEGSEM). Electron backscatter diffraction (EBSD) analysis was performed at an acceleration voltage of 25 kV using the Oxford INCA crystal software. Energy dispersive X-ray spectroscopy (EDS) was performed using the Oxford Energy software. Time-of-flight secondary ion mass spectroscopy (TOF-SIMS) was performed using an ionTOF ToF-SIMS5; elemental maps of the aged filaments were accumulated after sputtering the surface with oxygen ions. X-ray diffraction (XRD) patterns were collected in reflection geometry at 2θ-values ranging from 10–90° with a step size of 0.02°, using a PANalytical® XPe\rt diffractometer operated at 45 kV and 40 mA. Copper K_α radiation with a wavelength of 1.5406 Å was used as the X-ray source. The XRD patterns were indexed using the database maintained by the International Centre for Diffraction Data (ICDD) [5]. Vickers microhardness measurements were carried out using a FM-700® Microhardness Tester. Indentations were performed at a load of 0.05 kg and a dwell time of 10 s.

* Corresponding author. Tel.: +27 21 959 3473; fax: +27 21 959 3474.
E-mail address: cjarendse@uwc.ac.za (C.J. Arendse).

http://dx.doi.org/10.1016/j.tsf.2014.10.012
0040-6090/

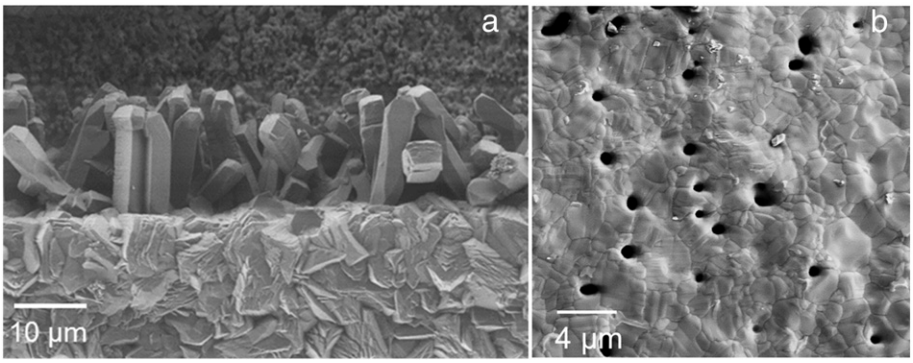

Fig. 1. SEM micrographs of the filament surface sampled from (a) ends closer to the contacts and (b) the centre regions.

3. Results and discussion

Fig. 1 presents SEM micrographs of the filament surface at the end and centre regions. At the cooler ends a solid silicon nitride layer according to EDS analysis (not shown here) covers the filament. In contrast, the silicon nitride layer is absent from the centre regions and porosity develops within the filament surface. Fig. 2 presents a backscatter electron micrograph of the end filament cross-section. The total filament diameter increased to 341.01 ± 10.17 μm. Cracks are also visible extending from the filament surface into the bulk. Secondary electron images (not shown here) revealed a solid silicon nitride layer encapsulating the filament. Nevertheless, distinct regions of contrast exist within and around the filament after the HWCVD of SiN_x. However, phase analysis based on contrast in a SEM backscatter image of aged filaments can be misleading considering that contrast differences can also be caused by grain orientation relative to the incident electron beam [6]. Analysing possible tantalum nitride or silicide regions by EDS is also unreliable (EDS analysis not shown here) given the large atomic number difference between Ta and N and the overlap between Ta and Si X-ray lines.

Fortunately, EBSD makes up for the current limitations of EDS in analysing the phases of an aged filament. The EBSD phase map shown in Fig. 2c identified eight phases namely (in decreasing order of prominence): Ta, Ta_2N, Ta_2Si, α-Ta_5Si_3, TaN, Ta_5Si_3 (metastable), Ta_3Si and β-Si_3N_4. The Ta-silicides are present at the outer perimeters of the filament. The outer silicon nitride layer did not show any Kikuchi patterns as it experienced considerable beam damage at an accelerating voltage of 25 kV. Lowering the accelerating voltage did not induce a detectable EBSD signal. As a result, it was not possible in the current system to perform EBSD of the outer silicon nitride layer.

The EBSD phase map shown in Fig. 2c discloses that the dark areas of contrast in the filament bulk are predominantly Ta_2N regions. Moreover, porosity is prevalent throughout the filament bulk, occupying spaces at grain boundaries and within the grains. The Ta_2N regions tend to form within Ta grains and especially at the Ta grain boundaries. Fig. 3 shows TOF-SIMS elemental maps of the aged filament sampled from the ends revealing the N, Ta and Si containing ions. The TOF-SIMS results corroborate with the EDS and SEM analyses on the presence of a silicon nitride layer on the filament surface. In addition, TOF-SIMS revealed that SiH and Si are prominent within the silicon nitride layer. The layer below the silicon nitride layer and the filament bulk contained regions of TaN and TaO_2. The TaO_2 probably formed as a result of sputtering the sample with O ions prior to the ToF-SIMS measurements.

Interestingly, there seems to be significant signals of H and TaH within the filament bulk, especially along cracks and within the SiN_x layer in the case of H. The areas rich in C corresponds to the resin used to mount the sample. During the deposition, the products of the dissociation process, i.e. the N and Si containing radicals diffuse into the heated Ta filament to form various silicides and nitrides depending on the concentration of N and Si atoms [7]. In addition, the diffusion lengths of H and N are expected to be larger than that of Si. Nitrogen and H will therefore diffuse more effectively into the filament bulk. The diffusion paths of the Si, N and H atoms are most likely along the Ta grain boundaries and cracks, which ultimately become preferred sites for Ta_2N formations and accumulation of H. Silicon will accumulate at the

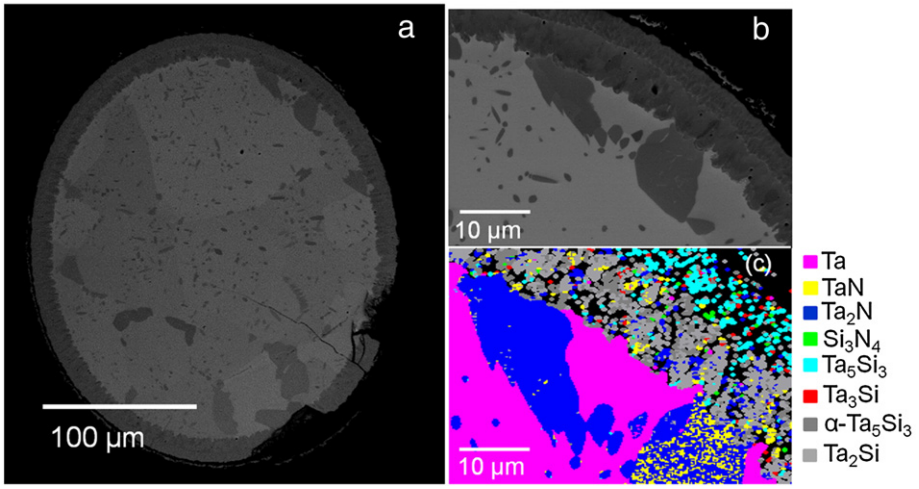

Fig. 2. Backscatter electron micrographs of (a) ends filament cross-section and (b) at a higher magnification, showing porosity. EBSD phase map (c) of the area shown in (b).